Biointerface Research in Applied Chemistry
Open-Access Journal (ISSN: 2069-5837)

Article
Volume 13, Issue 6, 2023, 544
https://doi.org/10.33263/BRIAC136.544

Green Approach to Corrosion Inhibition of Mild Steel in Hydrochloric Acidusing Extractfromthe Pericarp of the fruit *Tamarindus indica* (Tamarind)

Vinitha Pinto [1,†], Geetha M Pinto [1,*,†], Lavanya D Kateel [2], Asha Thomas [3]

[1] Department of Chemistry, St Agnes Centre for Postgraduate Studies and Research, Mangaluru - 575002, Karnataka, India
[2] Department of Chemistry, Canara Engineering College, Benjanapadavu -574219 and affiliated to Visvesvaraya Technological University, Belagavi, Karnataka – India;lavanyakateel@gmail.com
[3] Department of Chemistry, Providence Women's College, Uty of Calicut; mariaasha19@gmail.com
* Correspondence: geetha@stagnescollege.edu.in;
† First and second authors contributed equally to this study;

Scopus Author ID 35748889900
Received: 24.09.2022; Accepted: 6.11.2022; Published: 8.02.2023

Abstract: Plant materials are still employed for metal corrosion, which is a significant cause for concern, given their simplicity in synthesis, availability, accessibility, cost, environmental friendliness, and potent inhibitory action. This study treats mild steel in a hydrochloric acidic media with the pericarp of the *Tamarindus indica* fruit (TPW) as a green inhibitor. The aqueous extract of the reed of tamarind is rich in organic compounds determined using the peaks obtained from the UV-visible spectrum and IR spectrum. The inhibition efficiency of the extract is determined using weight loss and electrochemical methods. It was discovered that inhibition efficiency rises with increasing inhibitor concentrations but falls with rising temperatures and increasing acid media concentrations. The maximum inhibition efficiency was found to be 91.7% at 303 K in 0.25 M HCl. A mixed type of indicator is TPW, which obeys Langmuir adsorption Isotherms, and the inhibition mechanism is studied for the constituent molecules present in the TPW. In this study, mild steel in a hydrochloric acidic media is treated with the pericarp of the Tamarindus indica fruit (TPW) as a green inhibitor and the activation energy is calculated to study the inhibition mechanism. The sample surface morphology is analyzed using scanning electron microscopy and energy-dispersive x-ray spectroscopy.

Keywords: mild steel;corrosion;polarization;electrochemical impedance

1. Introduction

Materials around us use metals and their alloys for their structural applications. This is mainly because of the low cost and easy availability of metals needed for inventions, fabrications, and their desired mechanical properties. The applications of metals and their alloys are extended from building construction to bridges and dams, ornaments and automobiles, machinery, and so on, which brought about an industrial revolution in the modern era [1]. But these so-called useful metals face a constant and continuous problem as they are chemically and environmentally attacked [2].

Adding to this, industrial processes like acid washing result in unwanted metal corrosion [3]. The widely used methods against the corrosion of materials against the corroding

solutions and thus to protect them are many. But when an inhibitor is added to protect the metals, it has applications in acid pickling, industrial acid cleaning, acid descaling, cleaning of oil refinery equipment and oil well acidizing, etc. [4,5]. Thus it is necessary to add a small concentration of inhibitors to the corrosive media, which will decrease or prevent the reaction of metal with that corrosive medium. These inhibitors can be added to the cooling systems, refinery units, oil, gas production units, chemicals, boiler, etc., as they have a heteroatom like N, O, S and the multiple bonds in their molecules, which get adsorbed on the d orbital, of the metal surface [6].

But these inhibitors are toxic, costly, and environmentally destructive, so there is a need for green inhibitors which are environmentally friendly, cheap, and have good sustainable results [7]. Thus green chemistry appreciates the use of natural products as corrosion inhibitors due to their vast availability, pollution-free, and biodegradability [8-12]. The green inhibitors are organic compounds and follow the mechanism of adsorption on the metal surface. It may include the electrostatic interaction between the charged metal and the inhibitor molecule [13].

Thus the extracted compounds from natural products such as henna, honey, pectin, propolis, Tagetes erecta, Musa paradisical, and sabdariffa are used in acidic media [14-24]. Asha Thomas *et al*. have studied the corrosion inhibition properties of Garcinia indica extract in hydrochloric acid for mild steel and obtained an efficiency of 93% for 0.5M HCl, 87% for 1M HCl at 303K[25]. Jiyaul Haque investigated the corrosion inhibition of Thevtia Peruviana [26]. Mohammad Amin Bidi studied the inhibition efficiency of hyalomma tick extract and showed an increase in corrosion inhibition efficiency with the increase in inhibitor concentration [27]. Anti-corrosive properties of Q-235 steel were studied using the aqueous extract of Brassica oleracea in two acidic mediums of HCl and H_2SO_4 by Hao Li *et al*., showing the efficiency of 92.3% in H_2SO_4 and 93.8% in HCl [28]. Shimaa N. Ali examined the anti-corrosive properties of fenugreek seeds in HCl and H_2SO_4[29]. Sanjay Kumar *et al*. have displayed their work on the inhibitor of Azadirachta indica, popularly known as neem, in acidic media[30]. Piper longum extract is used as a green inhibitor against the corrosion of metal aluminum with basic medium NaOH by Ambrish Singh *et al*. [31]. Jasna Halambek *et al*. have evaluated the anti-corrosive properties of pectin isolated from tomato peel waste for natural tin corrosion using sodium chloride and acetic acid medium [32]. The inhibitory action from the leaves of Ananas sativum leaves for aluminum in acid hydrochloride solutions is found to be 96.09% in 0.5M acid using gravimetric and hydrogen evolution methods by E.I. Ating *et al*. [33]. J.O.Madu *et al*. have shown the inhibitor action of Terminalia Catappa leaves extract in an acidic medium for stainless steel, which is 96.8% [34]. Ali Dehghani *et al*. have screened to inhibitory efficiency of Tamarindus indica extract to be 93% by the EIS method for 800ppm concentration [35]. Sangeetha Jayakumar *et al*. investigated the efficiency of tamarind fruit pulp as a green inhibitor in an acidic medium of hydrochloride[36].

Similarly, Iroha and James have also discussed the green inhibition of tamarind fruit pulp perfural resin[37]. Khalid *et al*. used tamarind fruit leave to study their inhibitory efficiency against mild steel in an acidic medium[38]. Velvet tamarind fruit extract in sulphuric acid was used against aluminum corrosion inhibition by James A.O. *et al*. [39]. Osarulobe *et al*. have shown the green inhibition of African black velvet tamarind (Dialium indium) for mild steel and copper[40,41]. The tartaric acid obtained from purpald in 0.5M sulphuric acid has the inhibitor efficiency for mild steel by Guo *et al*. [42]. The tannin extracted from the tamarind shell in Nigeria using methanol was used for rust transformation and had an efficiency of 95.8%. In comparison, the aqueous acetone extract of Tamarind shell achieved rust

transformation of 94.8% for mild steel in acidic hydrochloride by Abdulmajid A. *et al*. [43]. Thus a lot of study on the various parts of Tamarindus indica has been done as a green inhibitor against corrosion to protect the metal. Tamarindus indica Linn is a leguminous plant species of Fabaceae, Leguminosae, or Caesalpiniaceae family. Tamarind is a Persian word that means 'Date of India'. Every part of the tamarind tree is useful as it is medicinal and antioxidant, adds nutrition and flavors to culinary preparations, and is cost-effective[44,45]. The present work discusses the inhibitory efficiency of the aqueous extract of Tamarindus indica pericarp (TPW) to avail for its industrial use. The reason to have TPW is that it is eco-friendly, cost-effective, and due to its availability. The aqueous extract of the entire pericarp of the tamarind fruit as an inhibitor is applied for the anti-corrosive action of metal is a novel idea. The basic knowledge of the resistance to corrosion by the TPW is carried out through gravimetric analysis. The effect of acid and inhibitor concentration, temperature, etc., is made using electrochemical methods such as EISand PDP. By obtaining the thermodynamic parameters, kinetic and adsorption studies of the inhibitor on metal were done, which shed light on the cathodic and anodic corrosion reactions. The impact made on the metal by TPW is obtained through morphological analysis.

2. Materials and Methods

2.1. Test solutions.

2.1.1. Medium/Electrolyte.

Hydrochloric acid (HCl) solution of different concentrations is obtained by diluting the HCl in distilled water.

2.1.2. TPW extract.

The aqueous extract of TPW with a concentration of 10% is obtained by refluxing the dried pericarp of Tamarindus indica for 3 hours at 90°C. This extract is kept overnight and filtered to obtain the stock solution. The corrosion inhibition studies were made by adding the stock solution into the electrolyte and thus obtained 1%, 2%, 3%, and 4%.

2.2. Electrodes.

The electrodes used for the electrochemical studies include a saturated calomel electrode (SCE) as a reference electrode, a platinum electrode as an auxiliary electrode, and the mild steel specimen as the working electrode. The composition of the mild steel taken was (0.8%) C, (0.1%) Si, (0.060) P, (0.080) S, and (98.6%) Fe. The area of the mild steel specimen used for EIS and PDP studies was 1.0 cm^2, and the area for the gravimetric analysis was 2.37 cm^2.

2.3. Characterization of TPW.

TPW used for the study is a plant extract containing many functional groups responsible for inhibiting metal corrosion. So these functional groups were detected using FT-IR and Double beam UV–Visible spectrometry. The UV-visible double beam spectroscopy determines the absorbance of the TPW extract, and FTIR peaks were recorded by scan, including wavelength range 4000-500cm^{-1}.

2.4. Gravimetric analysis.

The corrosion efficiency of tamarind rind is found in dilute hydrochloric acid of strength 0.5N and 1N. 1-4% of TPW was added to make up to 80ml. A beaker was placed separately with the acid itself as a blank solution. Mild steel specimens were polished with emery papers to mirror a bright finish. The bars were washed in water and dried, and each bar's weight was taken using an electronic balance. Then the bars were dipped in the solutions for 24 h. After 24 h, the bars were taken out, and the metal surface was washed with water and weighed using an electronic balance. By comparing the initial and final weight, the efficiency of the extract in inhibiting metal corrosion can be found using the weight loss method.

Equation (1) is used to calculate the % inhibitor efficiency of the weight loss method.

$$\text{Inhibitor efficiency } \%IE = \frac{\text{W inh} - \text{W uninh}}{\text{Winh}} \times 100 \quad (1)$$

where Winh and Wuninh are the weight loss values with and without different inhibitor concentrations, respectively.

The corrosion rate is measured using equation (2).

$$CR = \frac{W}{A \times t} \quad (2)$$

where W is the weight loss due to immersion, A is the area exposed, and t is the time taken in hours.

2.5. Electrochemical tests.

Electrochemical testing was performed in a three-electrode cell using an electrochemical corrosion analyzer model Gill AC 1864 from ACM instruments, UK connected to a computer. Each run was carried out in aerated solutions at the required temperature, using a thermostatically controlled water bath. The mild steel was immersed in the test solution for 10 minutes until the open circuit potential E was reached. The potentiodynamic current–potential curves were executed with respect to E_{corr}, with a scan rate of 60mV/min for recording the Tafel plots and the potential sweep of ± 250mV versus open circuit potential at different temperatures (303K, 313K, 323K & 333K). EIS measurements for recording the impedance spectrum at the open circuit potential are between the frequency ranges of 0.1Hz to 100kHz using AC signals of 10mV.

2.6. Surface analysis.

The influence of the phytochemical constituent of the extract on the corrosion phenomenon of the mild steel was detected by taking photographs of fresh inhibited and uninhibited mild steel samples, which were recorded using SEM-EDXS. Scanning Electron Microscope TESCAN VEGA3 was used for the analysis of the morphology of mild steel samples. For SEM and EDX analysis, metal coupons were prepared following the same procedure as explained for the gravimetric analysis.Themildsteelspecimenswereimmersedfor24hoursin1MHClsolutionwith and without 10% of TPW extract at 303K. After 24 hours, the mild steel was taken out of the test solution, rinsed with di-ionized water and ethanol, dried, and submitted for SEM and EDX.

3. Results and Discussion

3.1. Gravimetric studies.

3.1.1 Effect of immersion time.

The value obtained from the gravimetric analysis is given in Table 1.

Table 1. Values obtained from the gravimetric analysis.

Concentration of acid:	**0.5M HCl**		**1M HCl**	
Volume of the inhibitor (V/V%)	CR(mg/cm^2 h)	%IE	CR(mg/cm^{2}h)	%IE
Blank	0.8926		1.4437	
1%	0.3145	64.76	0.5455	62.21
2%	0.2882	67.72	0.5055	64.99
3%	0.2289	74.35	0.4269	70.43
4%	0.1777	80.09	0.2669	81.51
5%	0.0717	91.96	0.2222	84.61

The pH of the blank and after adding the TPW extract had no change. From the results obtained from the gravimetric analysis, it can be seen that as the TPW extract concentration increases, the corrosion rate decreases with the increase in inhibitor efficiency. It could be explained with regard to the active molecules of the TPW extract being absorbed on the active corroding sites of the mild steel. In spite of dipping the metal in the electrolyte for 24 hours, 4% TPW showed an efficiency of 91%, assuring the extract's effectiveness. However, there is a decrease in the efficiency with regard to the increase in the concentration of acid because of metal dissolution; with the increase in the concentration of the acid, the energy barrier for corrosion decreases, and the formation of the activated complex becomes easy leading to higher corrosion rate. A plot (Figure 1) of inhibitor efficiency versus TPW extract concentration shows the maximum efficiency by volume of 5%.

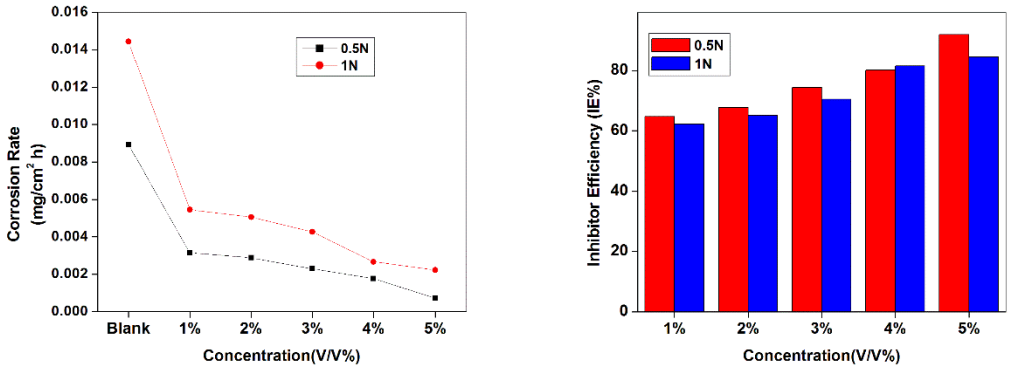

Figure 1. Results of weight loss studies of TPW extract.

3.2. Bode plots.

Figure 2 gives the Bode plot drawn by taking the log of the frequency versus phase angle shift. The electrode-electrolyte interface acts as an imperfect capacitor, as the phase angle deviates from 90°. Thus maximum deviation can be expected for blank, and as the concentration of TPW increases, the bode plot broadens. Figure 2b has a phase angle shift of 37.29 for blank, whereas as the concentration of TPW increases, the phase angle shift increases by 48.74 for 4% TPW extract, indicating the adsorption of TPW extract on the metal surface. At the same time, the bode plot of blank and the lower concentration of TPW in electrolyte

portrays the reduced capacitive response and hence the increased corrosion rate of mild steel in HCl. From Figure 2c, the Bode plot for the increase in temperature has no effect, but the deviation of the phase angle is more for higher temperatures of 333 K than 303K [46].

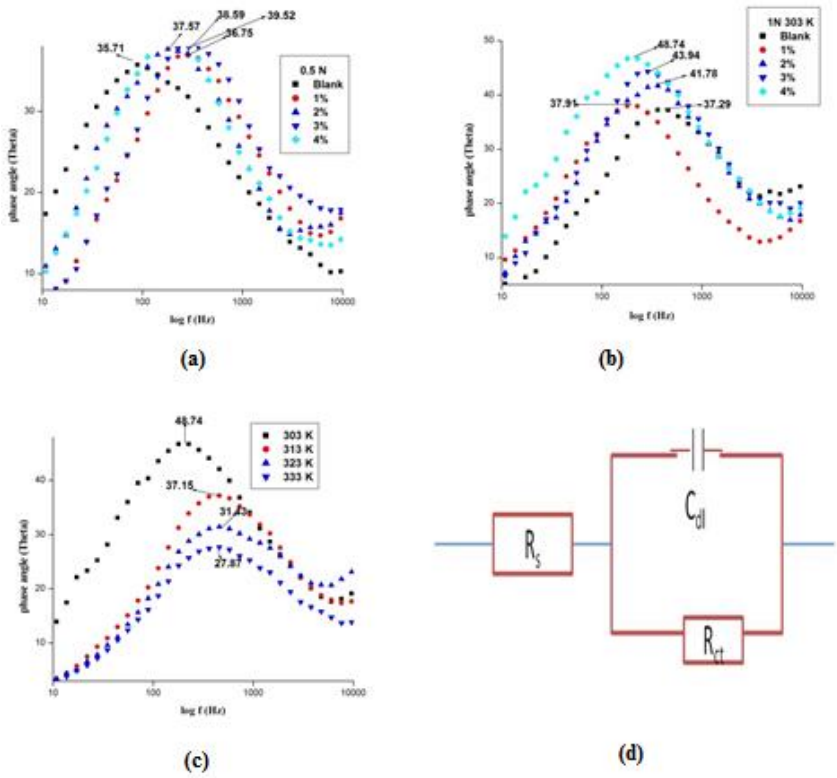

Figure 2. Bode plot for TPW at 303K (a)in 0.5M HCl (b) in1 M HCl (c)at different temperatures for 4% TPW extract (d) Equivalent circuit used to fit EIS data of TPW extract in 1 M HCl.

3.3. Analysis of EIS.

The impedance offered by the electrochemical system has elements like capacitance and resistance obtained from the electrochemical impedance spectra. Randle's circuit in Figure 2d is the simplest electrical equivalent circuit to explain the electrochemical behavior of the metal in an acidic solution. Here R_s stands for solution resistance, R_{ct} means charge transfer resistance, and C_{dl} is double-layer capacitance. From the output of EIS, the analysis plot can be drawn using the real part of the impedance along the X-axis, and the imaginary part is taken along the Y-axis. The difference between the real axis impedance at the initial and final frequencies gives the charge transfer resistance. The inhibitor efficiency can be calculated using equation (3):

$$\text{Inhibitor efficiency } IE\ \% = \frac{R_{ct_{inh}} - R_{ct_{uninh}}}{R_{ct_{inh}}} \times 100 \qquad (3)$$

where $R_{ct_{inh}}$ and $R_{ct_{uninh}}$ is the charge transfer resistance of the inhibited and blank respectively.

C_{dl} represents the double-layer capacitance resulting from a barrier to the current flow due to the ionic layer obtained from the metal solution interface, having ions from the metal, electrolyte, and TPW inhibitor. C_{dl} can be calculated by equation (4).

$$C_{dl} = \frac{1}{\omega(Rct)} \qquad (4)$$

where ωis the angular frequency given as 2πf and f is the frequency (Hz) where the imaginary part of the impedance has the maximum value and R_{ct} is the charge transfer resistance.

The corrosion inhibition is obtained by an increased concentration of inhibitor, which causes the thickness of the double layer to reduce the current flow [47].

3.3.1. Effect of TPW concentration.

The charge transfer resistance due to the presence of TPW extract for the temperatures of 303K, 313K, 323K, and 333K is seen through a Nyquist Plot of Figure 3. This figure shows that the diameter of the Nyquist Plot, the semicircles in the presence of the TPW extract, is higher than that of the blank solution [48]. So with the increased concentration of the extract which is adsorbed on the mild steel surface, a stable protecting film is formed on the metal surface [49]. The increase of impedance, at the increasing temperatures, increases the thickness of the electrical double layer on the metal electrolyte interface which is due to the adsorption of the greater number of constituent molecules of the extract, causing difficulty to mass and charge transfer process, which is essential for corrosion. Charge transfer resistance (Ohm/Cm^2), double layer capacitance (μF/cm^2), corrosion current density (mA/cm^2), and corrosion rate (mm/year) obtained from the EIS measurements are given in Table 2. From the results obtained from Table 2, it is clear that as the value of R_{ct} increases, C_{dl} decreases for all temperatures. R_{ct} value for the blank is 8.744, and for 4% is 44.49, and this increase is due to the adsorption of the inhibitor molecules on the metal surface. C_{dl} value for the blank is 4448, and for 4% is 1144, which shows that the double-layer capacitance value decreases due to the increase in the thickness of the double layer**.**

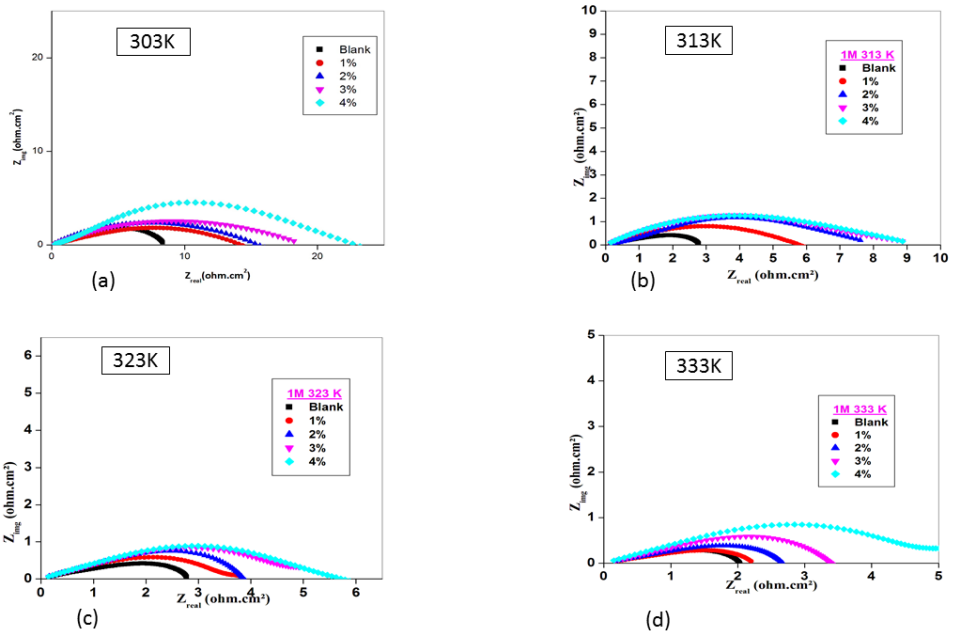

Figure 3. Nyquist plots for various concentrations of TPW extract in 1 M HCl at (a) 303 K (b)313 K (c)323 K (d) 333 K.

3.3.2. Effect of acid concentration.

The Nyquist plot Figure 4a is for 0.5M HCl, and Figure 3a is for 1M HCl; similarly, Figure 3b shows the Nyquist plot for 4% TPW extract in 0.25M, 0.5M, 1M, and 2M HCl acid concentration. This Nyquist plot has a single capacitive loop, and the radius of the capacitive loops decreases with an increase in the concentrations of acid for the increase in the

concentration of TPW extract along with the blank. The R_{ct} of 4% solution in 0.5M HCl is 136.7 in 1M HCl. which is reduced to 44.49. Thus, the activated complex formed due to the increased acid concentration is responsible for a higher corrosion rate. Semicircles of the Nyquist plot are imperfect due to the frequency dispersion.

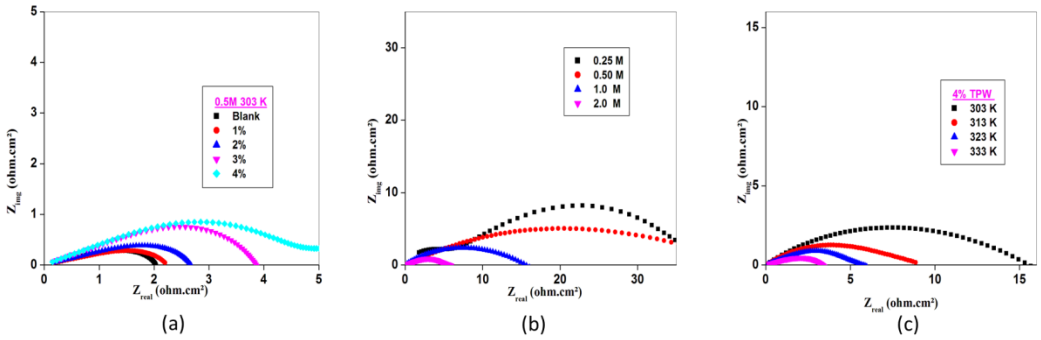

Figure 4. Nyquist plot (a) at various concentrations of TPW extract in 0.5 M HCl (b)4% TPW at different concentrations of HCl (c) 4% TPW at various temperatures in 1 M HCl.

3.3.3. Effect of temperature.

The Nyquist plot of Figure 4c shows the EIS studies for 4% TPW extract for temperatures 303K, 313K, 323K, and 333K. The diameter of the Nyquist plot is maximum at 303K and minimum at 333K. The R_{ct} value for 4% TPW extract at 303K is 44.49, reduced to 3.842 at 333K. Thus, it shows that as the temperature increases, the impedance increases, and the rate of corrosion increases. It is mainly because, with the temperature rise, the inhibitor molecules' desorption rate increases. The values in Table 2 indicate that the TPW extract is an efficient inhibitor despite higher temperatures.

Table 2. TPW extract as an efficient inhibitor.

Temp	Volume of TPW (V/V%)	R_{sol} (ohms.cm^2)	R_{ct} (ohms.cm^2)	C_{dl} (µF/cm^2)	I_{corr} (mA/cm^2)	C_R (mm/yr)	IE%
303 K	Blank	0.080	8.74	4448.5	2.98	34.6	
	1	0.071	18.35	3414.3	2.32	26.9	52.3
	2	0.371	22.26	2002.9	2.07	25.3	60.7
	3	0.180	30.07	1816.9	1.85	22.6	70.9
	4	0.126	44.49	1144.5	1.30	18.2	80.3
313K	Blank	0.070	5.12	7546.1	5.10	116.5	
	1	-0.017	9.10	7126.3	2.58	29.9	43.8
	2	0.099	11.27	2114.6	2.31	26.8	54.6
	3	0.007	13.69	2989.2	1.91	22.1	62.6
	4	-0.102	16.76	3005.9	1.32	18.0	69.5
323K	Blank	0.096	3.17	3214.9	8.23	95.4	
	1	0.062	4.58	2478.8	5.69	62.0	30.9
	2	0.015	5.39	1394.9	4.84	52.7	41.3
	3	0.032	7.27	2537.2	3.59	39.1	56.4
	4	0.044	8.03	1574.4	3.25	37.6	60.6
333K	Blank	0.099	1.95	3106.3	13.40	155.3	
	1	0.101	2.30	3015.9	11.32	131.2	15.5
	2	0.169	2.75	2323.2	9.50	110.1	29.1
	3	0.114	3.35	1284.5	7.34	85.1	41.9
	4	0.052	3.84	896.0	6.79	73.9	49.3
(0.5M) 303K	Blank	2.122	24.12	7912.9	1.08	11.8	
	1	-0.171	53.40	3505.0	0.49	5.7	54.8
	2	-0.442	69.42	1526.2	0.38	4.4	65.3
	3	-0.797	92.31	1316.0	0.28	3.3	73.9
	4	-0.417	136.70	1178.4	0.24	2.8	82.4

Temp	Volume of TPW (V/V%)	R_{sol} (ohms.cm^2)	R_{ct} (ohms.cm^2)	C_{dl} (µF/cm^2)	I_{corr} (mA/cm^2)	C_R (mm/yr)	IE%
(0.25M) 303K	Blank	1.132	12.67	1752.0	0.54	12.7	
	4	0.401	131.61	1503.0	6.38	7.4	90.4
(2M) 303K	Blank	0.162	11.67	7654.0	5.68	47.2	
	4	0.310	41.72	1236.0	6.25	7.2	72.0

3.4. Polarization studies.

The result of the different concentrations of TPW inhibitor on the cathodic and anodic action of mild steel in 0.5M HCl at room temperatures and 1M HCl for 303K, 313K, 323K, and 333K were analyzed. The resulting Tafel curves are given in Figure 5 and Figure 6a The current response of a sample for the applied potential is given the polarisation in the potentiometric polarization technique. It can be observed that by the addition of the TPW extract, the potential shifts toward more positive values and less current. The corrosion resistance of mild steel increases in the presence of the TPW inhibitor. The negative of E_{corr} values is the anodic curve, and positive values of E_{corr} give cathodic current.

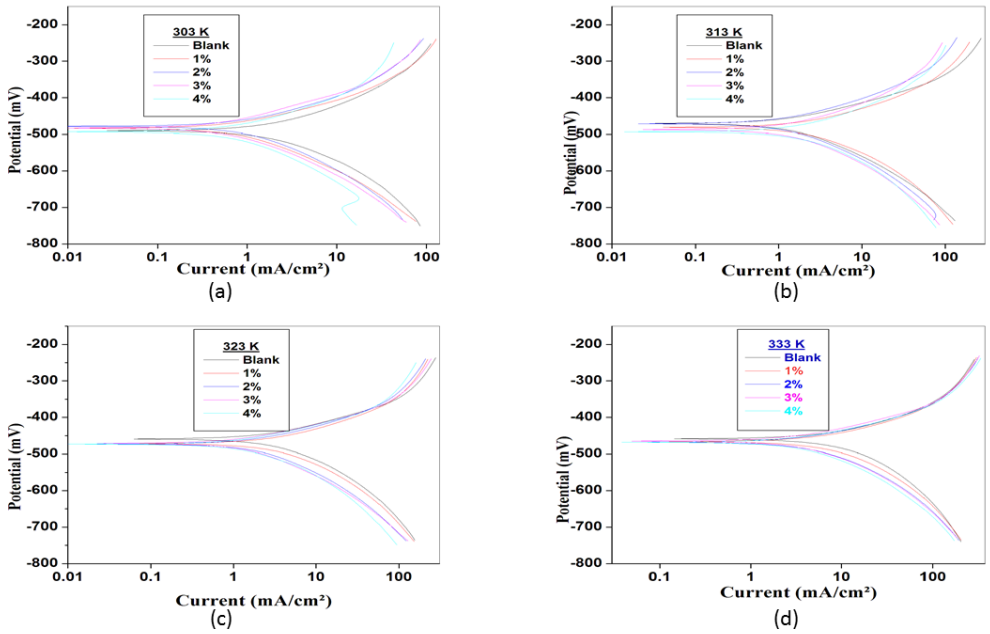

Figure 5. Tafel plots for various concentrations of TPW extract in 1 M HCl (a) 303 K; (b) 313 K; (c) 323 K; (d) 333K.

The linear portions of the polarization curve (stern diagram) were extrapolated until they intersected as straight lines, through which I_{corr} and E_{corr}, the Tafel constants, were calculated.

Table 3 shows the parameters studied in the polarization technique. There is no definite pattern for the E_{corr} values. Still, the low value of the difference between E_{corr} in blank and the inhibited solution confirms the mixed type of behavior of TPW extract, which affects both ionization of the anode, which is mild steel, and the cathodic hydrogen evolution. The less negative values of the E_{corr} for the solution containing TPW extract have the maximum effect on the anodic reaction by the inhibitor [50]. I_{corr} gives the corrosion current density, decreasing from 7.8525mA for the blank to 1.5513mA for 4% TPW extract at room temperature.

The Tafel plot displayed in Figure 6b for 4% solution at different temperatures shows that the I_{corr} values have risen from 1.5513mA to 14.454mA. This is due to the desorption of the constituent molecules as a protective layer on the metal surface with increasing energy or temperatures. Figure 6c shows the Tafel plot of 4% TPW extract for various concentrations, where it shows the efficiency of the TPW inhibitor in a lower concentration of the corrosive medium. The efficiency, calculated using equation (5), is relatively close to the calculated efficiency from the EIS measurements [51].

$$\text{Inhibitor efficiency } \%IE = \frac{I_{corr\ uninh} - I_{corr_{inh}}}{I_{corr\ uninh}} \times 100 \quad (5)$$

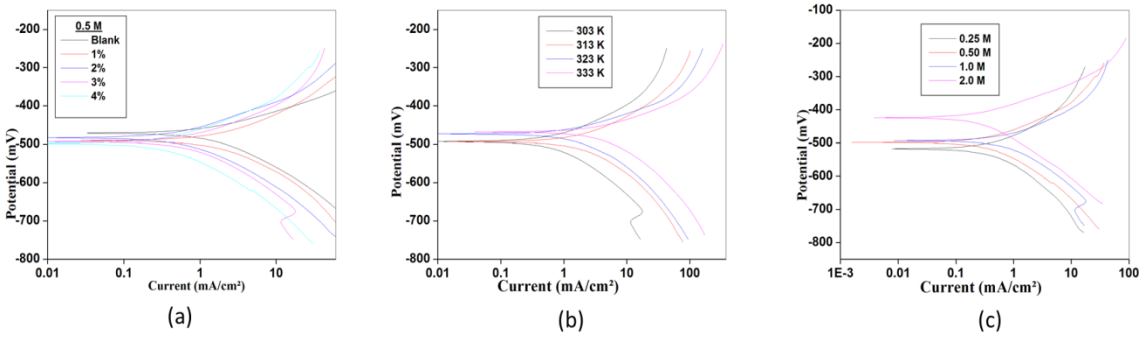

Figure 6. Tafel plot for (a) various concentrations of TPW extraction 0.5 M HCl (b)for 4% TPW at various temperatures in 1 M HCl (c) 4% TPW at different concentrations of HCl

By the addition of TPW extract to HCl, which is the corrosive medium, the βa and βc value changes, which shows that the inhibitor added controls the corrosion of mild steel, due to the dissolution of metals and evolution of hydrogen through the adsorption of the constituents of the inhibitor on the cathode and the anode which are the active sites. But the change in values of βc is considered more prominent thanβa, revealing the inhibitor is more cathodic.

Table 3. Parameters studied in the polarization technique.

Temp (K)	Volume of TPW (V/V%)	E_{corr} (mV)	β_a (mV)	-β_c(mV)	I_{corr} (mA/cm^2)	V_{corr} (mm/yr)	IE% (%)
303 K	Blank	489.93	127.0	140.3	7.853	92.82	
	1	483.96	80.6	130.0	3.775	62.89	51.9
	2	476.96	85.0	123.0	3.182	55.63	59.5
	3	482.13	102.3	134.7	2.537	45.54	67.7
	4	493.94	83.5	114.5	1.551	30.16	80.2
313K	Blank	480.64	119.1	160.6	13.408	158.48	
	1	492.49	77.1	90.3	6.814	123.47	49.2
	2	471.42	62.3	91.2	5.620	64.04	58.1
	3	470.38	68.0	90.0	4.712	58.87	64.9
	4	486.29	63.1	76.1	3.615	42.73	73.0
323K	Blank	472.76	108.4	164.5	11.318	133.78	
	1	458.43	64.5	84.0	9.770	127.30	13.7
	2	470.58	57.3	75.9	8.310	98.23	26.6
	3	472.19	52.8	84.4	8.138	96.19	28.1
	4	472.93	57.3	87.2	6.950	82.15	38.6
333K	Blank	458.9	90.6	106.5	17.324	204.77	
	1	468.4	82.4	100.3	16.208	191.58	6.4
	2	466.51	79.0	112.6	16.130	190.65	6.9
	3	464.93	70.1	100.2	14.671	173.42	15.3
	4	468.16	68.6	101.9	14.454	170.84	16.6
(0.5M) 303K	Blank	502.7	150.1	201.8	3.693	43.65	

Temp (K)	Volume of TPW (V/V%)	E_{corr} (mV)	β_a (mV)	-β_c(mV)	I_{corr} (mA/cm^2)	V_{corr} (mm/yr)	IE% (%)
	1	503.68	72.8	90.4	1.637	24.08	55.7
	2	492.68	90.1	117.8	1.317	20.53	64.3
	3	498.28	73.9	99.1	1.103	17.77	70.1
	4	495.58	68.2	95.5	0.810	15.55	78.1
(0.25M) 303K	Blank	504	149.0	223.9	16.525	138.83	
	4	519	106.2	163.4	1.369	16.18	91.7
(2M) 303K	Blank	412	97.7	187.1	11.856	137.54	
	4	423	66.9	127.6	3.229	38.17	72.8

Adsorption is a process of accumulating molecules on a surface by separating them from different phases. The organic inhibitors in a solution get adsorbed on the metal surface, and the water molecules from the metal surface substitute for the solution phase. Adsorption quantity on the metal surface or at the interface between the surface and the solution by the organic inhibitor mainly depends on the nature of the electric charge and the electrochemical potential at an interface or the metal surface, the chemical structure of the molecules present in the organic inhibitor, the chemical composition of the solution. Adsorption isotherms like Langmuir, Temkin, Frumkin, and Freundlich isotherms were obtained for the data of surface coverage (θ) and the Concentration C(V/V%). The following equations of the various isotherms give the link between the surface coverage (θ) and the Concentration C (V/V %) [52, 53].

$$\frac{C\ inh}{\theta} = C\ inh + \frac{1}{K\ ads} \quad \text{(Langmuir isotherm plot of } \frac{C\ inh}{\theta} \text{ Vs. } C_{inh}) \tag{6}$$

$$\theta = \frac{2.303}{\alpha}(\log K\ ads) + \log C \quad \text{(Temkin isotherm plot of } \theta \text{ Vs. log C)} \tag{7}$$

$$\frac{\theta}{1-\theta} = K\ ce^{2a\theta} \quad \text{(Frumkin isotherm plot of } \frac{\theta}{1-\theta} \text{ Vs. log C} \tag{8}$$

$$\log\theta = n\log C + \log K\ ads \quad \text{(Freundlich isotherm plot of log } \theta \text{ Vs. log C} \tag{9}$$

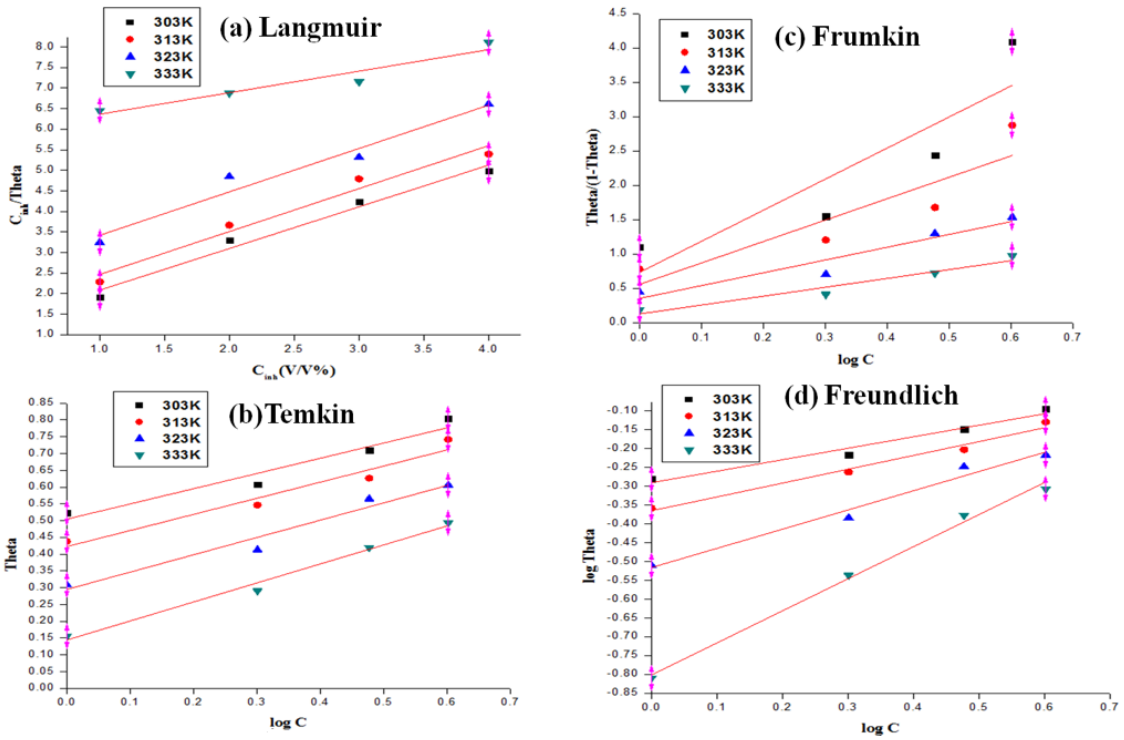

Figure 7. Adsorption isotherm for TPW extract at different temperatures in 1 M HCl.

Figure 7 gives the linear relationships for the isotherm of equations (6), (7), (8), and (9).R^2 values for the various isotherms are displayed in Table 4. The maximum regression

coefficient (R^2) is exhibited by the Langmuir isotherm, which almost equals 1. This shows that the Langmuir model could be chosen to analyze the adsorption process. The active sites are provided with equal surface energy by the Langmuir isotherm, which allows the single substituted layer of adsorbed molecules on the homogeneous surface without giving importance to the interaction of the individual molecules [54, 55]. The adsorption equilibrium constant (K_{ads}) is evaluated using the Langmuir plot. The relationship between $K_{ads}$and free energy adsorption is given in equation (10).

$$\Delta G^0 = -2.303RT \log (55.5\ K_{ads}) \quad (10)$$

where R represents the universal gas constant, and 55.5 is the concentration of water molecules in mol/L. the higher value of K_{ads} is a sign of the forward direction of the adsorption process.

The value of $\Delta G^{0,}$ which is -12kJ/mol, a negative value, not only confirms the spontaneity of the adsorption of molecules but also suggests the physisorption of the constituent molecules through electrostatic force of attraction between the positively charged metal surface and the electron-rich aromatic rings or by back donation of electrons by the metal surface to the molecules.

Figure 7a depicts the Langmuir isotherm, a straight line not passing from the origin, signifying the deviation from the ideal behavior of the TPW extract in the absorption process. The negative value of the enthalpy of adsorption in Table 4 confirms that the nature of the adsorption process is exothermic. The decrease of values in the entropy of adsorption proves that the adsorbed molecules are confined on the mild steel surface.

Table 4. The nature of the adsorption process is exothermic,

Temp (K)	**Langmuir C_{inh} Vs C_{inh}/θ**						**Frumkin θ/1-θ Vs logC**	**Temkin logC Vs θ**	**Freundlich logC Vs logθ**
	Slope	K_{ads}	R^2	ΔG^0 (kJ/mol)	ΔH^0ads (kJ/mol)	ΔS^0 ads (J/K mol)	R^2	R^2	R^2
303	1.15	2.8361	0.9905	-12.74	-9.60	23.58	0.8887	0.9711	0.9316
313	1.06	2.3615	0.9938	-12.69	-8.78	19.63	0.8831	0.9869	0.9990
323	1.05	2.2388	0.9823	-12.95	-8.75	18.61	0.9188	0.9432	0.9675
333	1.08	1.9687	0.9772	-12.99	-9.00	16.37	0.9706	0.9824	0.9920

3.6 Thermodynamic studies on the kinetics of corrosion inhibition.

The thermodynamic parameters of the corrosion inhibition are listed in table 5. It is the result of the study made by using the Arrhenius equation by plotting ln(CR) Vs. 1000/T and also the transition equation (Figure 8a). The logarithm of corrosion rate in an acidic solution is a linear function of 1/T, which is given in the Arrhenius type relation given in equation (11)[56].

$$\ln CR = \frac{-E_a}{2.303RT} + A \quad (11)$$

where E_a is the activation energy of the metal dissolution reaction, R is the universal Gas constant, and A is the Arrhenius pre-exponential factor.

The activation energy (E_a) has a higher value for the inhibited solution than the uninhibited solution, which confirms the adsorption of the constituent molecules on the mild steel surface. This adsorption causes a higher energy barrier for the corrosive acid molecules,

which would otherwise lead to corrosion in inhibited solutions. From Table 5, the E_a value greater than 20kJ/mol affirms physisorption, which is the surface process for corrosion inhibition.

The Transition state plots, which depict the plot of ln(CR/T) vs. 1/T, represent the equation (12).

$$CR = \frac{RT exp^{\frac{\Delta H}{RT}}}{Nh} \qquad (12)$$

where N is Avogadro's number, h is Planck's constant, ΔS is the activation entropy, and ΔH is the activation enthalpy.

The enthalpy of activation (ΔH_a) and the entropy of activation is obtained from the plot of ln(CR/T) vs. 1/T given in Figure 8b.

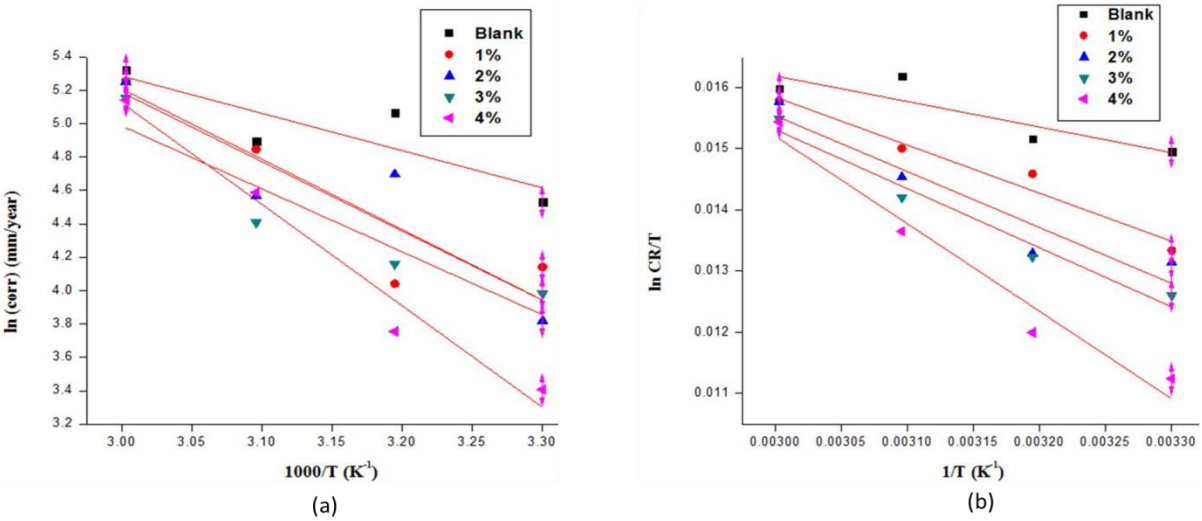

Figure 8. Arrhenius and transition state plot for TPW.

Metal dissolution has endothermic nature, which can be confirmed by the positive values of enthalpy of activation (ΔH_a). Mild steel dissolution can have a unimolecular mechanism as the difference between E_a, and ΔH_a is nearly equal to 2.52 kJ/mol, which holds good with the thermodynamic relation given in equation (13) [57,58].

$$E_a - \Delta H = RT \qquad (13)$$

The entropy of activation has more positive values (ΔS_a) in the inhibited solution assuring the formation of an activated complex during the rate-determining step since the disorder is more when the reactant is converted to its activated complex.

Table 5. Kinetic parameters of corrosion inhibition by TPW extract.

Arrhenius plot (1000/T Vs CR)		**Transition state plot**		**(lnCR/T Vs1/T)**
	E_a (kJ/mol)	ΔH_a (kJ/mol)	ΔS_a (kJ/mol)	E_a-ΔH_a (kJ/mol)
Blank	18.54	16.02	197.36	2.53
1%	34.50	31.97	207.20	2.53
2%	35.04	32.52	236.19	2.52
3%	31.31	28.78	278.23	2.53
4%	50.49	47.96	297.04	2.53

3.7. Surface morphology of test analysis.

3.7.1 SEM analysis.

Figure 9 gives the Scanning Electron Microscope (SEM) images of mild steel dipped in the blank with 4% TPW extract in 1M HCl for 24h. SEM analysis was done using Scanning Electron Microscope TESCAN VEGA3 to study the interaction of the metal surface with the constituent molecules. After immersion, the mild steel specimen was washed clean with distilled water and dried with acetone. In the absence of the extract Figure 9a, it was observed that the metal sample had a rough surface covered with a brown precipitate of iron oxide. But the sample in the presence of the extract had a smoother surface with considerably less damage. Figure 9b confirms the adsorption of the TPW extract on the surface of the metal by forming a protective layer on it, which is responsible for preventing the dissolution of mild steel in an acidic medium.

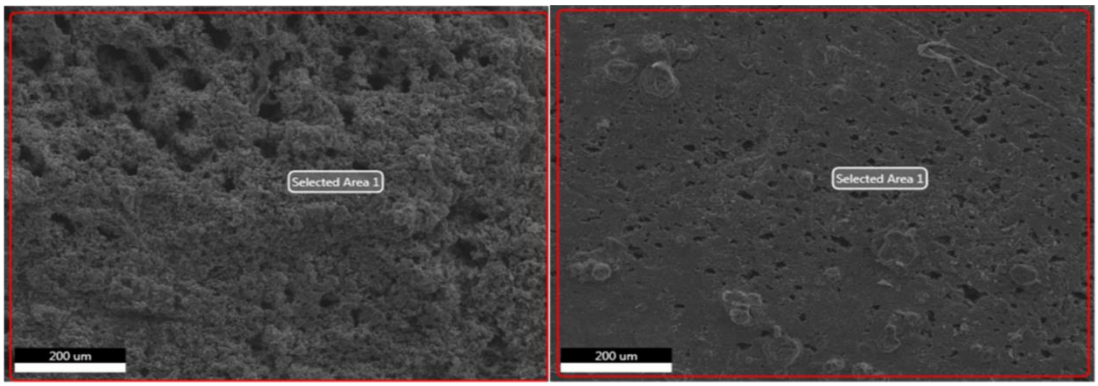

Figure 9. SEM image of mild steel sample in (a) immersed in 1 M HCl for 24 hours (b) immersed in 1 M HCl in the presence of 4% TPW extract for 24 hours.

3.7.2. Energy dispersive X-ray spectroscopy.

Figures 10a and 10b show the EDX images of the uninhibited and inhibited mild steel samples, respectively.

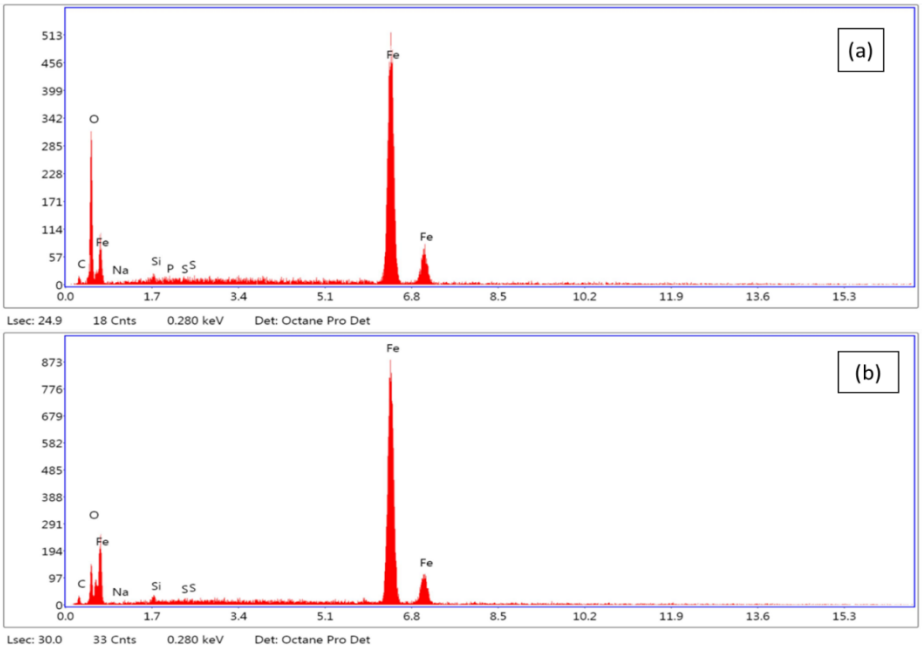

Figure 10. EDX spectra of mild steel sample in (a)immersed in 1 M HCl for 24 hours(b) immersed in 1 M HCl in the presence of 4% TPW extract for 24 hours.

The presence of an inhibitor reduces the oxygen peak considerably. The increase in the intensity of the iron peak, with the suppression of the oxygen peak, is due to the inhibitor protective film on the mild steel specimen. This affirms the adsorption of extract molecules on the surface of the mild steel forming a protective layer between the metal and the acid solution, which prevents metal dissolution in an aggressive medium [59-61]. Thus the addition of TPW extract has reduced the O/Fe, confirming the inhibitory action of TPW extract against the corrosion of mild steel in 1M HCl. Table 6 shows the higher percentage of Carbon content in the presence of the TPW than in the blank. At the same time, there is a decrease in the atomic percentage of iron in a blank solution, whereas, in the presence of the TPW extract, it increases. So the adsorption of molecules from the extract decreases the corrosion rate.

Table 6. EDX analysis data listing the percentage weight content of the elements.

Blank			**TPW**	
Element	Weight %	Atomic %	Weight %	Atomic %
C	4.43	11.64	8.20	21.94
O	25.05	47.23	9.51	21.44
Na	2.47	3.39	1.17	1.83
Si	0.18	0.20	0.62	0.8
S	0.27	0.26	0.12	0.11
Fe	67.24	36.32	80.7	52.14

3.8. Extract characterization.

3.8.1. FT-IR spectroscopy.

Figure 11 gives the IR spectrum of the TPW extract, which was done to find the functional groups present in the extract and to know their role as corrosion inhibitors for mild steel surfaces.

The peak of 3730.48 is due to the amide N-H stretch. The peak located at 3626.38 corresponds to the O-H stretching of alcohol. The peak of 1999.16 is assigned to C=C=C stretching as in allene and also C-H bending of aromatic compound. The peak that appeared at 1517.29 is attributed to the N-O stretching of a nitro compound, and the peak of 1219.25 is due to the C-O stretching of alkyl aryl ether. The peak of 1130.84 is the C-O stretching of ester or tertiary alcohol. The further peak of 1073.80 corresponds to the C-O stretching of primary alcohol. And the peak of 772.91 is located due to the C=C bending of tri-substituted alkenes. The peak of 681.64 is assigned to the C-Br stretching of the halo compound. The peak of 653.12 corresponds to the carbon having a single bond with a halo compound. The peak of 419.25 is located either due to C-Br or C-I starching mode. The existence of the functional group in the TPW extract indicates its anti-corrosive property to the metal surface.

3.8.2. UV- visible studies.

The organic extract forms complexes with the ions dissolved in the corrosive acid medium, which can be analyzed using the UV-visible spectrum [62]. UV-visible spectra of TPW given in Fig.12 gives the two broad absorption peaks between 200-260nm and 270-360nm. The band observed between 200-260nm is due to $n \rightarrow \sigma^*$transition. The band between 260-360nm corresponds to the $\pi \rightarrow \pi^*$transition of C=C, C=O, C≡C shows the presence of aliphatic dicarboxylic acids such as tannic acid, tartaric acid, and polyphenolic compounds such as tannin, proanthocyanidins. The UV visible spectrum of Fe ions in the presence of HCl and with TPW extract shows a decrease in the peak intensity at 387nm, as the organic molecules form a protective barrier on the surface of the mild steel through electron donation

and acceptance. The mild steel specimen in HCl containing the TPW extract shows a peak between 200nm to 240nm having n → π* and π → π* transition. The comparison between only TPW extract and TPW extract with metal ions shows the adsorbed organic molecules on mild steel, resulting in decreased peaks.

(a)

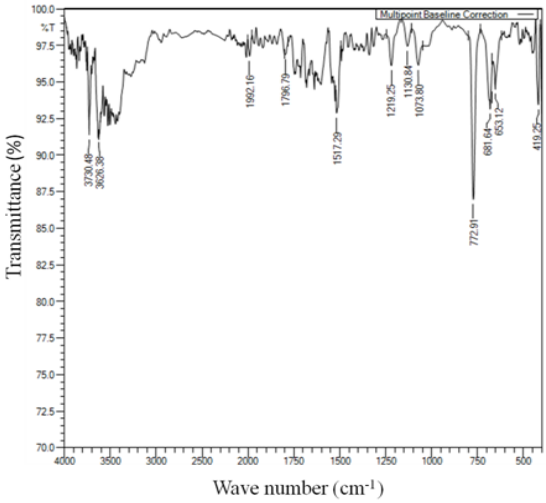

(b)

3730.48	Amide N-H stretch
3626.38	O-H stretching of alcohol
1999.16	C=C=C stretching as in allene and also C-H bending of aromatic compound
1517.29	The peak that appeared at 1517.29 is attributed to N O stretching of a nitro compound
1219.25	C-O starching of alkyl aryl ether
1130.84	C-O stretching of ester or tertiary Alcohol
1073.80	C-O stretching of primary alcohol
772.91	C=C bending of tri-substituted alkenes
681.64	C-Br stretching of halo compound
653.12	carbon having a single bond with a halo compound
419.25	C-Br or C-I starching mode

Figure 11. FTIR spectra of TPW extract (a) and corresponding values (b).

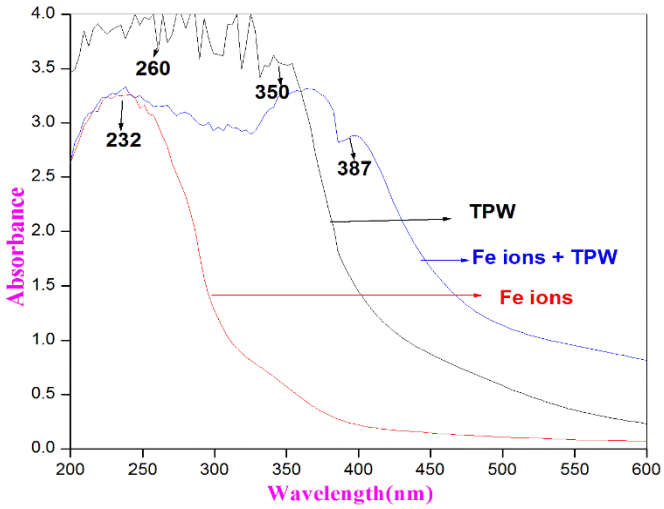

Figure 12. UV-Visible absorption spectra.

3.9. Mechanism of corrosion inhibition.

The anti-corrosive property of TPW extract as an inhibitor is studied here. The inhibition process on the mild steel, by the effective molecules present in the TPW extract, is

adsorbed on the metal surface to form a protective layer, replacing the water molecules. This is shown in equation (14).

$$\text{Inhibitor}_{(\text{Solution})} + \text{Water}_{(\text{adsorbed on metal})} \leftrightarrow \text{Water}_{(\text{Solution})} + \text{Inhibitor}_{(\text{adsorbed on metal})}$$

Metal dissolution occurs actively when there is an interface between corrosive acid and the metal. The metal surface can be protected from corrosion which mainly depends upon the concentration of the acid, environmental conditions, size of the molecules, adsorption centers as well as the chemical structure of the inhibitor. TPW extract is rich in organic molecules like polyphenolic compounds like tannin and proanthocyanidins etc. These phytochemicals contain hetero atoms like S, O, Na, and Si, which try to inhibit by reducing the metal dissolution process. The inhibition also depends upon the charge of the metal surface, which is the difference between the E_{corr} (Corrosion potential) and ZCP (Zero charge potential). When the difference between E_{corr} and ZCP is negative, the metal surface is negatively charged, attracting the positively charged molecules. Likewise, if the difference is positive, the metal surface will be positively charged, preferring negatively charged molecules. Mild steel in HCl is positively charged, which pre-adsorbs chloride anions on it [25, 35].

The inhibition mechanism of TPW extract is due to the electrostatic interaction between the mild steel surface and the organic molecules present in the extract. In addition, acceptor-donor interaction of Fe^{2+} and p-electrons of the heteroatoms of TPW takes place, adsorbing them on the metal surface. Thus, the complexes from the extract solution get attached to the mild steel surface through weak Van der Waals forces to build a physical barrier between the corrosive medium and the mild steel surface to reduce corrosion [63]. The reduction in anodic and cathodic Tafel slope values signifies the effectiveness of the TPW inhibitor in bringing down both the anodic iron dissolution and cathodic hydrogen evolution. Spectroscopic studies of FTIR, UV, and SEM, EDX analysis further confirm the adsorption of inhibitor molecules. TPW is cost-effective as it is an aqueous extract, unlike most green inhibitors, which are extracted using non-aqueous solvents that have toxic environmental effects. Therefore, TPW extract is an eco-friendly and renewable corrosion inhibitor for the protection of mild steel in an acidic medium such as HCl for the acid pickling and purification of mild steel, having a simple extraction process.

4. Conclusions

Tamarindus indica Pericarp water extract (TPW) is used as a corrosion inhibitor for mild steel in the HCl medium.TPW acts as an efficient green inhibitor against the corrosion of mild steel for different acid concentrations and temperatures. An efficiency of 91% is found in 0.25M HCl, and 80% efficiency is shown for 1M HCl concentration at 303K. EIS results showed an elevated charge transfer resistance upon increasing the concentration of TPW. The Potentiodynamic studies reveal the mixed type of behavior of the TPW extract, and it follows the Langmuir isotherm adsorption model for its adsorption on the metal surface. SEM and EDX analysis showed a physical barrier of the extract against corrosion of the metal surface. The negative value ΔG^0 suggests the stability of the adsorbed layer on the mild steel surface and the TPW extract adsorbed spontaneously on the mild steel surface.

FTIR and UV visible spectroscopy analysis indicated that the extract molecules were adsorbed on the mild steel surface to form a protective layer. Theoretical calculations assist the adsorption of TPW constituents on the metal surface by donating the electrons of the oxygen

or aromatic rings, engaging in back donation between the constituent molecules and the metal-centered orbital. The further study aims at separating the TPW extract to find out the active and reactive molecules present in it.

Funding

This research received no external funding.

Acknowledgments

Declared none.

Conflicts of Interest

The authors declare no conflict of interest.

References

1. Odusote, J.K.; Asafa, T.B.; Oseni, J.G.; Adeleke, A.A.; Adediran, A.A.; Yahya, R.A.; Abdul, J.M.; Adedayo, S.A. Inhibition efficiency of gold nanoparticles on corrosion of mild steel, stainless steel and aluminium in 1M HCl solution. *Mater. Today: Proc*. **2021**, *1*, 578-83, https://doi.org/10.1016/j.matpr.2020.02.984.
2. Obot, I.B.; Obi-Egbedi, N.O. Adsorption properties and inhibition of mild steel corrosion in sulphuric acid solution by ketoconazole: experimental and theoretical investigation. *Corros. Sci.* **2010**, *52*, 198-204,https://doi.org/10.1016/j.corsci.2009.09.002.
3. Dehghani, A.; Bahlakeh, G.; Ramezanzadeh, B.; Ramezanzadeh, M. Aloysia citrodora leaves extract corrosion retardation effect on mild-steel in acidic solution: Molecular/atomic scales and electrochemical explorations. *J. Mol. Liq.***2020,** *310*,113221,https://doi.org/10.1016/j.molliq.2020.113221.
4. Olusegun, S.J.; Adeiza, B.A.; Bodunrin, M.O.; Ikeke, K.I. Jatropha curcas leaves extract as corrosion inhibitor for mild steel in 1M hydrochloric acid. *j. emerg. trends eng. appl. sci.* **2013,** *4*, 138-43,https://hdl.handle.net/10520/EJC135989.
5. Rani, B.E.; Basu, B.B. Green inhibitors for corrosion protection of metals and alloys: an overview. *Int. J. Corros.* **2012**, *2012*, https://doi.org/10.1155/2012/380217.
6. Lavanya, D.K.; Frank ,V.P.; Vijaya, D.P.; Bangera, S. Inhibition effect of thiourea derivative for mild steel corrosion in acid medium: experimental and theoretical studies. *J. Bio- Tribo-Corros.* **2021**, *7*, 1-5, https://doi.org/10.1007/s40735-021-00487-7.
7. Miralrio, A.; Espinoza Vázquez, A. Plant extracts as green corrosion inhibitors for different metal surfaces and corrosive media: a review. *Process.* **2020,** *8*, 942, https://doi.org/10.3390/pr8080942.
8. Sannaiah, P.N.; Alva, V.D.; Bangera, S. An integrated electrochemical and theoretical approach on the potency of Senegalia rugata leaf extract as a novel inhibitor for mild steel in acidic medium. *J. Appl. Electrochem*. **2022**, *52*,395-412, https://doi.org/10.1007/s10800-021-01631-4.
9. Pavithra, N.S.; Alva, V.D.; Bangera, S. A sustainable and green approach to corrosion inhibition of mild steel by rangoon creeper flower extract in 1 M HCl. *Surf. Eng. Appl. Electrochem.* **2021**, *57*, 455-465, https://doi.org/10.3103/S106837552104013X.
10. Bangera, S.; Alva, V.D.; Pavithra, N.S. Averrhoa bilimbi leaf extract as a potent and sustainable inhibitor for mild steel in 1 M HCl medium: experimental and DFT enumeration. *Chemistry Africa*, **2022**, *5*, 341-358, https://doi.org/10.1007/s42250-022-00313-8.
11. Sannaiah, P.N.; Alva, V.D.P.;Bangera, S. An experimental, theoretical, and spectral approach to evaluating the effect of eco-friendly Oxalis stricta leaf extract on the corrosion inhibition of mild steel in 1 N H_2SO_4 medium. *J. Iran. Chem. Soc.* **2022,** *19*, 1817-1835, https://doi.org/10.1007/s13738-021-02422-6.
12. Hossain, N.; Asaduzzaman Chowdhury, M.; Kchaou, M. An overview of green corrosion inhibitors for sustainable and environment friendly industrial development. *J Adhes Sci Technol*. **2021**, *35*, 673-90, https://doi.org/10.1080/01694243.2020.1816793.
13. Hassannejad, H.; Nouri, A. Sunflower seed hull extract as a novel green corrosion inhibitor for mild steel in HCl solution.*J. Mol. Liq.* **2018**, *254*, 377-82, https://doi.org/10.1016/j.molliq.2018.01.142.

14. Radojčić, I.; Berković, K.; Kovač, S.; Vorkapić-Furač, J.J. Natural honey and black radish juice as tin corrosion inhibitors. *Corros. Sci.* **2008**, *50*, 1498-504, https://doi.org/10.1016/j.corsci.2008.01.013.
15. Molina-Ocampo, L.B.; Valladares-Cisneros, M.G.; Gonzalez-Rodriguez, J.G. Using Hibiscus sabdariffa as corrosin inhibitor for Al in 0.5 M H_2SO_4. *Int J Electrochem Sci.* **2015**, *10*, 388-403, http://www.electrochemsci.org/papers/vol10/100100388.pdf.
16. Parthipan, P.; Narenkumar, J.; Elumal, P.; Preethi, P.S.; Nanthin, A.U.; Agrawal, A.; Rajasekar, A. Neem extract as a green inhibitor for microbiologically influenced corrosion of carbon steel API 5LX in a hypersaline environments. *J. Mol. Liq.* **2017**, *240*,121-7, https://doi.org/10.1016/j.molliq.2017.05.059.
17. Varvara, S.; Bostan, R.; Bobis, O.; Găină, L.; Popa, F.; Mena, V.; Souto, R.M. Propolis as a green corrosion inhibitor for bronze in weakly acidic solution. *Appl. Surf. Sci* .**2017**, *426*, 1100-12,https://doi.org/10.1016/j.apsusc.2017.07.230.
18. Fares, M.M.; Maayta, A.K.; Al-Qudah, M.M. Pectin as promising green corrosion inhibitor of aluminum in hydrochloric acid solution. *Corros. Sci.***2012**,*60*,112-7,https://doi.org/10.1016/j.corsci.2012.04.002.
19. Mourya, P.; Banerjee, S.; Singh, M.M. Corrosion inhibition of mild steel in acidic solution by Tagetes erecta (Marigold flower) extract as a green inhibitor. *Corros. Sci.***2014,***85*, 352-63, https://doi.org/10.1016/j.corsci.2014.04.036.
20. Verma, C.; Ebenso, E.E.; Bahadur, I.; Obot, I.B.; Quraishi, M.A. 5-(Phenylthio)-3H-pyrrole-4-carbonitriles as effective corrosion inhibitors for mild steel in 1 M HCl: experimental and theoretical investigation. *J. Mol. Liq.* **2015**, *212*, 209-18, https://doi.org/10.1016/j.molliq.2015.09.009.
21. Ostovari, A.; Hoseinieh, S.M.; Peikari, M.; Shadizadeh, S.R.; Hashemi, S.J. Corrosion inhibition of mild steel in 1 M HCl solution by henna extract: A comparative study of the inhibition by henna and its constituents (Lawsone, Gallic acid, α-d-Glucose and Tannic acid). *Corros. Sci*. **2009,** *51*, 1935-49, https://doi.org/10.1016/j.corsci.2009.05.024.
22. Ji, G.; Anjum, S.; Sundaram, S.; Prakash, R. Musa paradisica peel extract as green corrosion inhibitor for mild steel in HCl solution. *Corros. Sci.* **2015**, *90*, 107-17, https://doi.org/10.1016/j.corsci.2014.10.002.
23. Arenas, M.A.; Conde, A.; De Damborenea, J.J. Cerium: a suitable green corrosion inhibitor for tinplate. *Corros. Sci.* **2002**, *44*, 511-20, https://doi.org/10.1016/S0010-938X(01)00053-1.
24. Sin, H.L.;Rahim, A.A.; Gan, C.Y.; Saad, B.; Salleh, M.I.; Umeda, M. Aquilaria subintergra leaves extracts as sustainable mild steel corrosion inhibitors in HCl. Measurement **2017**, *109*, 334-45, https://doi.org/10.1016/j.measurement.2017.05.045.
25. Thomas, A.; Prajila, M.; Shainy, K.M.; Joseph, A. A green approach to corrosion inhibition of mild steel in hydrochloric acid using fruit rind extract of Garcinia indica (Binda). *J. Mol. Liq.* **2020**, *312*, 113369, https://doi.org/10.1016/j.molliq.2020.113369.
26. Haque, J.; Verma, C.; Srivastava, V.; Nik, W.W. Corrosion inhibition of mild steel in 1M HCl using environmentally benign Thevetia peruviana flower extracts. *Sustain. Chem. Pharm.* **2021**, *19*, 100354, https://doi.org/10.1016/j.scp.2020.100354.
27. Bidi, M.A.; Azadi, M.; Rassouli, M. A new green inhibitor for lowering the corrosion rate of carbon steel in 1 M HCl solution: Hyalomma tick extract. *Mater. Today Commun.* **2020**, *24*, 100996, https://doi.org/10.1016/j.mtcomm.2020.100996.
28. Li, H.; Qiang, Y.; Zhao, W.; Zhang, S. A green Brassica oleracea L extract as a novel corrosion inhibitor for Q235 steel in two typical acid media. *Colloids Surf. A Physicochem. Eng. Asp.* **2021**, *616*, 126077, https://doi.org/10.1016/j.colsurfa.2020.126077.
29. Al LEHAIBI, H.A. Control of zinc corrosion in acidic media: green fenugreek inhibitor. rans. Nonferrous Met. Soc. China **2016**, *26*, 3034-45, https://doi.org/10.1016/S1003-6326(16)64434-5.
30. Sharma, S.K.; Mudhoo, A.; Jain, G.; Khamis, E. Corrosion inhibition of Neem (Azadirachta indica) leaves extract as a green corrosion inhibitor for Zinc in H_2SO_4. *Green Chem Lett Rev.* **2009,** *2*, 47-51, https://doi.org/10.1080/17518250903002335.
31. Singh, A.; Ahamad, I.; Quraishi, M.A. Piper longum extract as green corrosion inhibitor for aluminium in NaOH solution. *Arab. J. Chem.* **2016**, *9*, S1584-9, https://doi.org/10.1016/j.arabjc.2012.04.029.
32. Halambek, J.; Cindrić, I.; Grassino, A.N. Evaluation of pectin isolated from tomato peel waste as natural tin corrosion inhibitor in sodium chloride/acetic acid solution. *Carbohydr. Polym.* **2020**, *234*, 115940, https://doi.org/10.1016/j.carbpol.2020.115940.
33. Ating, E.I.; Umoren, S.A.; Udousoro, I.I.; Ebenso, E.E.; Udoh, A.P.; Leaves extract of Ananas sativum as green corrosion inhibitor for aluminium in hydrochloric acid solutions. *Green Chem Lett Rev.* **2010**, *3*, 61-8, https://doi.org/10.1080/17518250903505253.

34. Madu, J.O.; Ifeakachukw,C.; Okorodudu, U.; Adams, F.V.; Joseph, I.V. Corrosion Inhibition Efficiency of Terminalia Catappa Leaves Extracts on Stainless Steel in Hydrochloric Acid. *J. Phys. Conf. Ser.* **2019**, *1378*, 022092, https://iopscience.iop.org/article/10.1088/1742-6596/1378/2/022092/meta.
35. Dehghani, A.; Bahlakeh, G.; Ramezanzadeh, B.; Ramezanzadeh, M. Electronic/atomic level fundamental theoretical evaluations combined with electrochemical/surface examinations of Tamarindus indiaca aqueous extract as a new green inhibitor for mild steel in acidic solution (HCl 1 M). *J Taiwan Inst Chem Eng*. **2019**, *102*,349-77, https://doi.org/10.1016/j.jtice.2019.05.006.
36. Jayakumar, S.; Nandakumar, T.; Vadivel, M.; Thinaharan, C.; George, R.P.; Philip, J. Corrosion inhibition of mild steel in 1 M HCl using Tamarindus indica extract: electrochemical, surface and spectroscopic studies. *J Adhes Sci Technol* **2020**, *34*, 713-43, https://doi.org/10.1080/01694243.2019.1681156.
37. Iroha, N.B.; James, A.O. Assessment of performance of velvet tamarind-furfural resin as corrosion inhibitor for mild steel in acidic solution. *Journal of Chemical Society of Nigeria.* **2018**, *43*, https://www.journals.chemsociety.org.ng/index.php/jcsn/article/view/199.
38. Khalid, K.I.; Sylvester, O.D.; Okoro, L.N. Corrosion inhibition of mild steel in formic acid using Tamarindus indica extract. *Res J Chem Sci.* **2016**, *6*, 32-35.
39. James, A.O.; Osarolube, E. Inhibition of aluminum corrosion in 0.5 M sulphuric acid solutions by velvet tamarind-water extract. *Int. j. sci. eng.* **2015,** *6*, 1537-47.
40. Eziaku, O.; James, A.O. Corrosion inhibition of mild steel in hydrochloric acid by African black velvet tamarind. *j. emerg. trends eng. appl. sci.* **2014**, *5*, 51-5.
41. Osarolube, E.; James, A.O. Corrosion inhibition of copper using African black velvet tamarind (Dialium indium) extract in sulphuric acid environment. *J. Sci. Res. Rep.* **2014**, *3*, 2450-8, https://doi.org/10.9734/JSRR/2014/9434.
42. Guo, L.; Wu, M.; Leng, S.; Qiang, Y.; Zheng, X. Synergistic effect of purpald with tartaric acid on the corrosion inhibition of mild steel: From electrochemical to theoretical insights. *Prot. Met. Phys. Chem.* **2018,** *54*, 917-25, https://doi.org/10.1134/S2070205118050076.
43. Abdulmajid, A.; Hamidon, T.S.; Rahim, A.A.; Hussin, M.H. Tamarind shell tannin extracts as green corrosion inhibitors of mild steel in hydrochloric acid medium. *Mater. Res. Express* **2019,** *6*, 106579, https://iopscience.iop.org/article/10.1088/2053-1591/ab3b87/meta.
44. Devi, B.; Boruah, T. Tamarind (Tamarindus indica). InAntioxidants in Fruits: *Properties and Health Benefits* **2020**, 317-332. Springer, Singapore, https://doi.org/10.1007/978-981-15-7285-2_16.
45. Abdelnaby, A.; Abdel-Aleem. N.; Mansour, A.; Abdelkader, A.; Ibrahim, A.N.; Sorour, S.M.; Elgendy, E.; Bayoumi, H.; Abdelrahman, S.M.; Ibrahim, S.; Alsaati, I. The combination of Tamarindus indica and coenzyme Q10 can be a potential therapy preference to attenuate cadmium-induced hepatorenal injury. *Front. Pharmacol.* **2022,** 2716, https://doi.org/10.3389/fphar.2022.954030.
46. Singh, A.; Ansari, K.R.; Haque, J.; Dohare, P.; Lgaz, H.; Salghi, R.; Quraishi, M.A. Effect of electron donating functional groups on corrosion inhibition of mild steel in hydrochloric acid: Experimental and quantum chemical study. *J Taiwan Inst Chem Eng* **2018**, *82*, 233-51, https://doi.org/10.1016/j.jtice.2017.09.021.
47. Khaled, K.; Abdel-Rehim, S.S. Electrochemical investigation of corrosion and corrosion inhibition of iron in hydrochloric acid solutions. *Arab. J. Chem.* **2011**, *4*, 397-402, https://doi.org/10.1016/j.arabjc.2010.07.006.
48. Chaouiki, A.; Lgaz, H; Chung, I.M.; Ali, I.H.; Gaonkar, S.L.; Bhat, K.S.; Salghi, R.; Oudda, H.; Khan, M.I. Understanding corrosion inhibition of mild steel in acid medium by new benzonitriles: insights from experimental and computational studies. *J. Mol. Liq.* **2018**, *266*, 603-16, https://doi.org/10.1016/j.molliq.2018.06.103.
49. Huang, L.; Wang, Z.M.; Wang, S.S.; Wang, Y.H.; Li, H.J.; Wu, Y.C. Environmentally benign cinchonain IIa from Uncaria laevigata for corrosion inhibition of Q235 steel in HCl corrosive medium: Experimental and theoretical investigation. *Environ. Res.* **2022**, 114376, https://doi.org/10.1016/j.envres.2022.114376.
50. Olasunkanmi, L.O.; Obot, I.B.; Kabanda, M.M.; Ebenso, E.E. Some quinoxalin-6-yl derivatives as corrosion inhibitors for mild steel in hydrochloric acid: experimental and theoretical studies. *J. Phys. Chem. C.* **2015**, *119*, 16004-19, https://doi.org/10.1021/acs.jpcc.5b03285.
51. Karki, N.; Neupane, S.; Gupta, D. K.; Das, A. K.; Singh, S.; Koju, G. M.; Yadav, A. P. Berberine isolated from Mahonia nepalensis as an eco-friendly and thermally stable corrosion inhibitor for mild steel in acid medium. *Arab J Chem.* **2021**, *14*, 103423, https://doi.org/10.1016/j.arabjc.2021.103423.

52. Aralu, C.C.; Chukwuemeka-Okorie, H.O.; Akpomie, K.G. Inhibition and adsorption potentials of mild steel corrosion using methanol extract of Gongronema latifoliuim. *Appl. Water Sci.* **2021**, *11*, 1-7, https://doi.org/10.1007/s13201-020-01351-8.
53. Ogunleye, O.O.; Arinkoola, A.O.; Eletta, O.A.; Agbede, O.O.; Osho, Y.A.; Morakinyo, A.F.; Hamed, J.O. Green corrosion inhibition and adsorption characteristics of Luffa cylindrica leaf extract on mild steel in hydrochloric acid environment. *Heliyon* **2020,** *6*, p.e03205. https://doi.org/10.1016/j.heliyon.2020.e03205.
54. Erami, R.S.; Amirnasr, M.; Meghdadi, S.; Talebian, M.; Farrokhpour, H.; Raeissi, K. Carboxamide derivatives as new corrosion inhibitors for mild steel protection in hydrochloric acid solution. *Corros. Sci.* **2019**, *151*, 190-7, https://doi.org/10.1016/j.corsci.2019.02.019.
55. Ammal, P.R.; Prajila, M.; Joseph, A. Physicochemical studies on the inhibitive properties of a 1, 2, 4-triazole Schiff's base, HMATD, on the corrosion of mild steel in hydrochloric acid. *Egypt. J. Pet.* **2018**, *27*, 307-17, https://doi.org/10.1016/j.ejpe.2017.05.002.
56. Fouda, A. E. A. S.; Abd El-Maksoud, S. A.; El-Sayed, E. H.; Elbaz, H. A.; Abousalem, A. S. Experimental and surface morphological studies of corrosion inhibition on carbon steel in HCl solution using some new hydrazide derivatives. *RSC Adv.* **2021**, *11*, 13497-13512, https://doi.org/10.1039/D1RA01405F.
57. Hamdy, A.; El-Gendy, N.S. Thermodynamic, adsorption and electrochemical studies for corrosion inhibition of carbon steel by henna extract in acid medium. *Egypt. J. Pet.* **2013,** *22*, 17-25, https://doi.org/10.1016/j.ejpe.2012.06.002.
58. Stern, M.; Geary, A.L. Electrochemical polarization: I. A theoretical analysis of the shape of polarization curves. *J. Electrochem. Soc.* **1957**, *104*, 56, https://iopscience.iop.org/article/10.1149/1.2428496/meta.
59. Jafar Mazumder, M.A. New, amino acid based zwitterionic polymers as promising corrosion inhibitors of mild steel in 1 M HCl. *Coatings* .**2019**, *9*, 675, https://doi.org/10.3390/coatings9100675.
60. Kavitha, N.; Ravichandran, J.; Murugesh, A. An eco-friendly Leucas aspera leaves extract inhibitor for copper corrosion in hydrochloric acid medium. *J. Bio- Tribo-Corros.* **2020**, *6*, 1, https://doi.org/10.1007/s40735-020-00400-8.
61. Meshram, Y.K.; Gunjate, J.K.; Khope, R.U. Studies on adsorption characteristics of manganese onto coal based chemically modified activated carbon. *Mater. Today: Proc.* **2020**, *29*, 1185-91, https://doi.org/10.1016/j.matpr.2020.05.428.
62. Rbaa, M.; Benhiba, F.; Hssisou, R.; Lakhrissi, Y.; Lakhrissi, B.; Touhami, M.E.; Warad, I.; Zarrouk, A. Green synthesis of novel carbohydrate polymer chitosan oligosaccharide grafted on d-glucose derivative as bio-based corrosion inhibitor. *J. Mol. Liq.* **2021,** *322*, 114549, https://doi.org/10.1016/j.molliq.2020.114549.
63. Muthukrishnan, P.; Jeyaprabha, B.; Prakash, P. Adsorption and corrosion inhibiting behavior of Lannea coromandelica leaf extract on mild steel corrosion. *Arab. J. Chem.* **2017**, *10*, S2343-54, https://doi.org/10.1016/j.arabjc.2013.08.011.